2009

Limit on the diffuse flux of ultrahigh energy tau neutrinos with the surface detector of the Pierre Auger Observatory

PHYSICAL REVIEW D, NEW YORK, v.79, 2009
http://producao.usp.br/handle/BDPI/16582

Limit on the diffuse flux of ultrahigh energy tau neutrinos with the surface detector of the Pierre Auger Observatory

J. Abraham,[7] P. Abreu,[63] M. Aglietta,[48] C. Aguirre,[11] E. J. Ahn,[78] D. Allard,[27] I. Allekotte,[1] J. Allen,[81] P. Allison,[83] J. Alvarez-Muñiz,[70] M. Ambrosio,[43] L. Anchordoqui,[93] S. Andringa,[63] A. Anzalone,[47] C. Aramo,[43] S. Argirò,[46] K. Arisaka,[86] F. Arneodo,[49] F. Arqueros,[67] T. Asch,[34] H. Asorey,[1] P. Assis,[63] J. Aublin,[29] M. Ave,[87] G. Avila,[9] T. Bäcker,[38] D. Badagnani,[5] K. B. Barber,[10] A. F. Barbosa,[13] S. L. C. Barroso,[18] B. Baughman,[83] P. Bauleo,[76] J. J. Beatty,[83] T. Beau,[27] B. R. Becker,[90] K. H. Becker,[32] A. Bellétoile,[30] J. A. Bellido,[10,84] S. BenZvi,[92] C. Berat,[30] P. Bernardini,[42] X. Bertou,[1] P. L. Biermann,[35] P. Billoir,[29] O. Blanch-Bigas,[29] F. Blanco,[67] C. Bleve,[42] H. Blümer,[37,33] M. Boháčová,[87,24] C. Bonifazi,[29,13] R. Bonino,[48] J. Brack,[76] P. Brogueira,[63] W. C. Brown,[77] R. Bruijn,[72] P. Buchholz,[38] A. Bueno,[69] R. E. Burton,[74] N. G. Busca,[27] K. S. Caballero-Mora,[37] L. Caramete,[35] R. Caruso,[45] W. Carvalho,[15] A. Castellina,[48] O. Catalano,[47] L. Cazon,[87] R. Cester,[46] J. Chauvin,[30] A. Chiavassa,[48] J. A. Chinellato,[16] A. Chou,[78,81] J. Chudoba,[24] J. Chye,[80] R. W. Clay,[10] E. Colombo,[2] R. Conceição,[63] B. Connolly,[91] F. Contreras,[8] J. Coppens,[57,59] A. Cordier,[28] U. Cotti,[55] S. Coutu,[84] C. E. Covault,[74] A. Creusot,[65] A. Criss,[84] J. Cronin,[87] A. Curutiu,[35] S. Dagoret-Campagne,[28] K. Daumiller,[33] B. R. Dawson,[10] R. M. de Almeida,[16] M. De Domenico,[45] C. De Donato,[41] S. J. de Jong,[57] G. De La Vega,[7] W. J. M. de Mello Junior,[16] J. R. T. de Mello Neto,[21] I. De Mitri,[42] V. de Souza,[15] G. Decerprit,[27] L. del Peral,[68] O. Deligny,[26] A. Della Selva,[43] C. Delle Fratte,[44] H. Dembinski,[36] C. Di Giulio,[44] J. C. Diaz,[80] P. N. Diep,[94] C. Dobrigkeit,[16] J. C. D'Olivo,[56] P. N. Dong,[94] D. Dornic,[26] A. Dorofeev,[79] J. C. dos Anjos,[13] M. T. Dova,[5] D. D'Urso,[43] I. Dutan,[35] M. A. DuVernois,[88] R. Engel,[33] M. Erdmann,[36] C. O. Escobar,[16] A. Etchegoyen,[2] P. Facal San Luis,[87,70] H. Falcke,[57,60] G. Farrar,[81] A. C. Fauth,[16] N. Fazzini,[78] F. Ferrer,[74] A. Ferrero,[2] B. Fick,[80] A. Filevich,[2] A. Filipčič,[64,65] I. Fleck,[38] S. Fliescher,[36] C. E. Fracchiolla,[14] E. D. Fraenkel,[58] W. Fulgione,[48] R. F. Gamarra,[2] S. Gambetta,[39] B. García,[7] D. García Gámez,[69] D. Garcia-Pinto,[67] X. Garrido,[33,28] G. Gelmini,[86] H. Gemmeke,[34] P. L. Ghia,[26,48] U. Giaccari,[42] M. Giller,[62] H. Glass,[78] L. M. Goggin,[93] M. S. Gold,[90] G. Golup,[1] F. Gomez Albarracin,[5] M. Gómez Berisso,[1] P. Gonçalves,[63] M. Gonçalves do Amaral,[22] D. Gonzalez,[37] J. G. Gonzalez,[69,79] D. Góra,[37,61] A. Gorgi,[48] P. Gouffon,[15] S. Grebe,[57,38] M. Grigat,[36] A. F. Grillo,[49] Y. Guardincerri,[4] F. Guarino,[43] G. P. Guedes,[17] J. Gutiérrez,[68] J. D. Hague,[90] V. Halenka,[25] P. Hansen,[5] D. Harari,[1] S. Harmsma,[58,59] J. L. Harton,[76] A. Haungs,[33] M. D. Healy,[86] T. Hebbeker,[36] G. Hebrero,[68] D. Heck,[33] C. Hojvat,[78] V. C. Holmes,[10] P. Homola,[61] J. R. Hörandel,[57] A. Horneffer,[57] M. Hrabovský,[25,24] T. Huege,[33] M. Hussain,[65] M. Iarlori,[40] A. Insolia,[45] F. Ionita,[87] A. Italiano,[45] S. Jiraskova,[57] M. Kaducak,[78] K. H. Kampert,[32] T. Karova,[24] P. Kasper,[78] B. Kégl,[28] B. Keilhauer,[33] E. Kemp,[16] R. M. Kieckhafer,[80] H. O. Klages,[33] M. Kleifges,[34] J. Kleinfeller,[33] R. Knapik,[76] J. Knapp,[72] D.-H. Koang,[30] A. Krieger,[2] O. Krömer,[34] D. Kruppke,[32] D. Kuempel,[32] N. Kunka,[34] A. Kusenko,[86] G. La Rosa,[47] C. Lachaud,[27] B. L. Lago,[21] M. S. A. B. Leão,[20] D. Lebrun,[30] P. Lebrun,[78] J. Lee,[86] M. A. Leigui de Oliveira,[20] A. Lemiere,[26] A. Letessier-Selvon,[29] M. Leuthold,[36] I. Lhenry-Yvon,[26] R. López,[50] A. Lopez Agüera,[70] J. Lozano Bahilo,[69] A. Lucero,[48] R. Luna García,[51] M. C. Maccarone,[47] C. Macolino,[40] S. Maldera,[48] D. Mandat,[24] P. Mantsch,[78] A. G. Mariazzi,[5] I. C. Maris,[37] H. R. Marquez Falcon,[55] D. Martello,[42] J. Martínez,[51] O. Martínez Bravo,[50] H. J. Mathes,[33] J. Matthews,[79,85] J. A. J. Matthews,[90] G. Matthiae,[44] D. Maurizio,[46] P. O. Mazur,[78] M. McEwen,[68] R. R. McNeil,[79] G. Medina-Tanco,[56] M. Melissas,[37] D. Melo,[46] E. Menichetti,[46] A. Menshikov,[34] R. Meyhandan,[58] M. I. Micheletti,[2] G. Miele,[43] W. Miller,[90] L. Miramonti,[41] S. Mollerach,[1] M. Monasor,[67] D. Monnier Ragaigne,[28] F. Montanet,[30] B. Morales,[56] C. Morello,[48] J. C. Moreno,[5] C. Morris,[83] M. Mostafá,[76] S. Mueller,[33] M. A. Muller,[16] R. Mussa,[46] G. Navarra,[48] J. L. Navarro,[69] S. Navas,[69] P. Necesal,[24] L. Nellen,[56] C. Newman-Holmes,[78] D. Newton,[72] P. T. Nhung,[94] N. Nierstenhoefer,[32] D. Nitz,[80] D. Nosek,[23] L. Nožka,[24] J. Oehlschläger,[33] A. Olinto,[87] V. M. Olmos-Gilbaja,[70] M. Ortiz,[67] F. Ortolani,[44] N. Pacheco,[68] D. Pakk Selmi-Dei,[16] M. Palatka,[24] J. Pallotta,[3] G. Parente,[70] E. Parizot,[27] S. Parlati,[49] S. Pastor,[66] M. Patel,[72] T. Paul,[82] V. Pavlidou,[87] K. Payet,[30] M. Pech,[24] J. Pękala,[61] R. Pelayo,[54] I. M. Pepe,[19] L. Perrone,[42] R. Pesce,[39] E. Petermann,[89] S. Petrera,[40] P. Petrinca,[44] A. Petrolini,[39] Y. Petrov,[76] J. Petrovic,[59] C. Pfendner,[92] A. Pichel,[6] R. Piegaia,[4] T. Pierog,[33] M. Pimenta,[63] T. Pinto,[66] V. Pirronello,[45] O. Pisanti,[43] M. Platino,[2] J. Pochon,[1] V. H. Ponce,[1] M. Pontz,[38] P. Privitera,[87] M. Prouza,[24] E. J. Quel,[3] J. Rautenberg,[32] D. Ravignani,[2] A. Redondo,[68] S. Reucroft,[82] B. Revenu,[31] F. A. S. Rezende,[13] J. Ridky,[24] S. Riggi,[45] M. Risse,[32] C. Rivière,[30] V. Rizi,[40] C. Robledo,[50] G. Rodriguez,[44] J. Rodriguez Martino,[45] J. Rodriguez Rojo,[8] I. Rodriguez-Cabo,[70] M. D. Rodríguez-Frías,[68] G. Ros,[67,68] J. Rosado,[67] M. Roth,[33] B. Rouillé-d'Orfeuil,[27] E. Roulet,[1] A. C. Rovero,[6] F. Salamida,[40] H. Salazar,[50] G. Salina,[44] F. Sánchez,[56] M. Santander,[8] C. E. Santo,[63] E. M. Santos,[21] F. Sarazin,[75] S. Sarkar,[71] R. Sato,[8] N. Scharf,[36] V. Scherini,[32] H. Schieler,[33] P. Schiffer,[36] A. Schmidt,[34] F. Schmidt,[87] T. Schmidt,[37] O. Scholten,[58] H. Schoorlemmer,[57,59] J. Schovancova,[24] P. Schovánek,[24] F. Schroeder,[33] S. Schulte,[36]

F. Schüssler,[33] D. Schuster,[75] S. J. Sciutto,[5] M. Scuderi,[45] A. Segreto,[47] D. Semikoz,[27] M. Settimo,[42] R. C. Shellard,[13,14] I. Sidelnik,[2] B. B. Siffert,[21] N. Smetniansky De Grande,[2] A. Smiałkowski,[62] R. Šmída,[24] B. E. Smith,[72] G. R. Snow,[89] P. Sommers,[84] J. Sorokin,[10] H. Spinka,[73,78] R. Squartini,[8] E. Strazzeri,[28] A. Stutz,[30] F. Suarez,[2] T. Suomijärvi,[26] A. D. Supanitsky,[56] M. S. Sutherland,[83] J. Swain,[82] Z. Szadkowski,[62] A. Tamashiro,[6] A. Tamburro,[37] T. Tarutina,[5] O. Taşcău,[32] R. Tcaciuc,[38] D. Tcherniakhovski,[34] N. T. Thao,[94] D. Thomas,[76] R. Ticona,[12] J. Tiffenberg,[4] C. Timmermans,[59,57] W. Tkaczyk,[62] C. J. Todero Peixoto,[16] B. Tomé,[63] A. Tonachini,[46] I. Torres,[50] P. Travnicek,[24] D. B. Tridapalli,[15] G. Tristram,[27] E. Trovato,[45] V. Tuci,[44] M. Tueros,[5] R. Ulrich,[33] M. Unger,[33] M. Urban,[28] J. F. Valdés Galicia,[56] I. Valiño,[70] L. Valore,[43] A. M. van den Berg,[58] V. van Elewyck,[26] R. A. Vázquez,[70] D. Veberič,[65,64] A. Velarde,[12] T. Venters,[87] V. Verzi,[44] M. Videla,[7] L. Villaseñor,[55] S. Vorobiov,[65] L. Voyvodic,[78] H. Wahlberg,[5] P. Wahrlich,[10] O. Wainberg,[2] D. Warner,[76] A. A. Watson,[72] S. Westerhoff,[92] B. J. Whelan,[10] G. Wieczorek,[62] L. Wiencke,[75] B. Wilczyńska,[61] H. Wilczyński,[61] C. Wileman,[72] M. G. Winnick,[10] H. Wu,[28] B. Wundheiler,[2,87] P. Younk,[76] G. Yuan,[79] E. Zas,[70] D. Zavrtanik,[65,64] M. Zavrtanik,[64,65] I. Zaw,[81] A. Zepeda,[52,53] and M. Ziolkowski[38]

(Pierre Auger Collaboration)

[1]*Centro Atómico Bariloche and Instituto Balseiro (CNEA- UNCuyo-CONICET), San Carlos de Bariloche, Argentina*
[2]*Centro Atómico Constituyentes (Comisión Nacional de Energía Atómica/CONICET/UTN-FRBA), Buenos Aires, Argentina*
[3]*Centro de Investigaciones en Láseres y Aplicaciones, CITEFA and CONICET, Argentina*
[4]*Departamento de Física, FCEyN, Universidad de Buenos Aires y CONICET, Argentina*
[5]*IFLP, Universidad Nacional de La Plata and CONICET, La Plata, Argentina*
[6]*Instituto de Astronomía y Física del Espacio (CONICET), Buenos Aires, Argentina*
[7]*Observatorio Meteorologico Parque Gral. San Martin (UTN- FRM/CONICET/CNEA), Mendoza, Argentina*
[8]*Pierre Auger Southern Observatory, Malargüe, Argentina*
[9]*Pierre Auger Southern Observatory and Comisión Nacional de Energía Atómica, Malargüe, Argentina*
[10]*University of Adelaide, Adelaide, S.A., Australia*
[11]*Universidad Catolica de Bolivia, La Paz, Bolivia*
[12]*Universidad Mayor de San Andrés, Bolivia*
[13]*Centro Brasileiro de Pesquisas Fisicas, Rio de Janeiro, RJ, Brazil*
[14]*Pontifícia Universidade Católica, Rio de Janeiro, RJ, Brazil*
[15]*Universidade de Sao Paulo, Instituto de Fisica, Sao Paulo, SP, Brazil*
[16]*Universidade Estadual de Campinas, IFGW, Campinas, SP, Brazil*
[17]*Universidade Estadual de Feira de Santana, Brazil*
[18]*Universidade Estadual do Sudoeste da Bahia, Vitoria da Conquista, BA, Brazil*
[19]*Universidade Federal da Bahia, Salvador, BA, Brazil*
[20]*Universidade Federal do ABC, Santo André, SP, Brazil*
[21]*Universidade Federal do Rio de Janeiro, Instituto de Física, Rio de Janeiro, RJ, Brazil*
[22]*Universidade Federal Fluminense, Instituto de Fisica, Niterói, RJ, Brazil*
[23]*Charles University, Faculty of Mathematics and Physics, Institute of Particle and Nuclear Physics, Prague, Czech Republic*
[24]*Institute of Physics of the Academy of Sciences of the Czech Republic, Prague, Czech Republic*
[25]*Palacký University, Olomouc, Czech Republic*
[26]*Institut de Physique Nucléaire d'Orsay (IPNO), Université Paris 11, CNRS-IN2P3, Orsay, France*
[27]*Laboratoire AstroParticule et Cosmologie (APC), Université Paris 7, CNRS-IN2P3, Paris, France*
[28]*Laboratoire de l'Accélérateur Linéaire (LAL), Université Paris 11, CNRS-IN2P3, Orsay, France*
[29]*Laboratoire de Physique Nucléaire et de Hautes Energies (LPNHE), Universités Paris 6 et Paris 7, Paris Cedex 05, France*
[30]*Laboratoire de Physique Subatomique et de Cosmologie (LPSC), Université Joseph Fourier, INPG, CNRS-IN2P3, Grenoble, France*
[31]*SUBATECH, Nantes, France*
[32]*Bergische Universität Wuppertal, Wuppertal, Germany*
[33]*Forschungszentrum Karlsruhe, Institut für Kernphysik, Karlsruhe, Germany*
[34]*Forschungszentrum Karlsruhe, Institut für Prozessdatenverarbeitung und Elektronik, Germany*
[35]*Max-Planck-Institut für Radioastronomie, Bonn, Germany*
[36]*RWTH Aachen University, III. Physikalisches Institut A, Aachen, Germany*
[37]*Universität Karlsruhe (TH), Institut für Experimentelle Kernphysik (IEKP), Karlsruhe, Germany*
[38]*Universität Siegen, Siegen, Germany*
[39]*Dipartimento di Fisica dell'Università and INFN, Genova, Italy*
[40]*Università dell'Aquila and INFN, L'Aquila, Italy*
[41]*Università di Milano and Sezione INFN, Milan, Italy*
[42]*Dipartimento di Fisica dell'Università del Salento and Sezione INFN, Lecce, Italy*
[43]*Università di Napoli "Federico II" and Sezione INFN, Napoli, Italy*

[44]*Università di Roma II "Tor Vergata" and Sezione INFN, Roma, Italy*
[45]*Università di Catania and Sezione INFN, Catania, Italy*
[46]*Università di Torino and Sezione INFN, Torino, Italy*
[47]*Istituto di Astrofisica Spaziale e Fisica Cosmica di Palermo (INAF), Palermo, Italy*
[48]*Istituto di Fisica dello Spazio Interplanetario (INAF), Università di Torino and Sezione INFN, Torino, Italy*
[49]*INFN, Laboratori Nazionali del Gran Sasso, Assergi (L'Aquila), Italy*
[50]*Benemérita Universidad Autónoma de Puebla, Puebla, Mexico*
[51]*Centro de Investigacion en Computo del IPN, México, D.F., Mexico*
[52]*Centro de Investigación y de Estudios Avanzados del IPN (CINVESTAV), México, D.F., Mexico*
[53]*Instituto Nacional de Astrofisica, Optica y Electronica, Tonantzintla, Puebla, Mexico*
[54]*Unidad Profesional Interdisciplinaria de Ingenieria y Tecnologia Avanzadas del IPN, Mexico, D.F., Mexico*
[55]*Universidad Michoacana de San Nicolas de Hidalgo, Morelia, Michoacan, Mexico*
[56]*Universidad Nacional Autonoma de Mexico, Mexico, D.F., Mexico*
[57]*IMAPP, Radboud University, Nijmegen, Netherlands*
[58]*Kernfysisch Versneller Instituut, University of Groningen, Groningen, Netherlands*
[59]*NIKHEF, Amsterdam, Netherlands*
[60]*ASTRON, Dwingeloo, Netherlands*
[61]*Institute of Nuclear Physics PAN, Krakow, Poland*
[62]*University of Łódź, Łódz, Poland*
[63]*LIP and Instituto Superior Técnico, Lisboa, Portugal*
[64]*J. Stefan Institute, Ljubljana, Slovenia*
[65]*Laboratory for Astroparticle Physics, University of Nova Gorica, Slovenia*
[66]*Instituto de Física Corpuscular, CSIC-Universitat de València, Valencia, Spain*
[67]*Universidad Complutense de Madrid, Madrid, Spain*
[68]*Universidad de Alcalá, Alcalá de Henares (Madrid), Spain*
[69]*Universidad de Granada & C.A.F.P.E., Granada, Spain*
[70]*Universidad de Santiago de Compostela, Spain*
[71]*Rudolf Peierls Centre for Theoretical Physics, University of Oxford, Oxford, United Kingdom*
[72]*School of Physics and Astronomy, University of Leeds, United Kingdom*
[73]*Argonne National Laboratory, Argonne, Illinois, USA*
[74]*Case Western Reserve University, Cleveland, Ohio, USA*
[75]*Colorado School of Mines, Golden, Colorado, USA*
[76]*Colorado State University, Fort Collins, Colorado, USA*
[77]*Colorado State University, Pueblo, Colorado, USA*
[78]*Fermilab, Batavia, Illinois, USA*
[79]*Louisiana State University, Baton Rouge, Louisiana, USA*
[80]*Michigan Technological University, Houghton, Michigan, USA*
[81]*New York University, New York, New York, USA*
[82]*Northeastern University, Boston, Massachusetts, USA*
[83]*Ohio State University, Columbus, Ohio, USA*
[84]*Pennsylvania State University, University Park, Pennsylvania, USA*
[85]*Southern University, Baton Rouge, Louisiana, USA*
[86]*University of California, Los Angeles, California, USA*
[87]*University of Chicago, Enrico Fermi Institute, Chicago, Illinois, USA*
[88]*University of Hawaii, Honolulu, Hawaii, USA*
[89]*University of Nebraska, Lincoln, Nebraska, USA*
[90]*University of New Mexico, Albuquerque, New Mexico, USA*
[91]*University of Pennsylvania, Philadelphia, Pennsylvania, USA*
[92]*University of Wisconsin, Madison, Wisconsin, USA*
[93]*University of Wisconsin, Milwaukee, Wisconsin, USA*
[94]*Institute for Nuclear Science and Technology (INST), Hanoi, Vietnam*
(Received 2 March 2009; published 1 May 2009)

Data collected at the Pierre Auger Observatory are used to establish an upper limit on the diffuse flux of tau neutrinos in the cosmic radiation. Earth-skimming ν_τ may interact in the Earth's crust and produce a τ lepton by means of charged-current interactions. The τ lepton may emerge from the Earth and decay in the atmosphere to produce a nearly horizontal shower with a typical signature, a persistent electromagnetic component even at very large atmospheric depths. The search procedure to select events induced by τ decays against the background of normal showers induced by cosmic rays is described. The method used to compute the exposure for a detector continuously growing with time is detailed. Systematic un-

certainties in the exposure from the detector, the analysis, and the involved physics are discussed. No τ neutrino candidates have been found. For neutrinos in the energy range 2×10^{17} eV $< E_\nu < 2 \times 10^{19}$ eV, assuming a diffuse spectrum of the form E_ν^{-2}, data collected between 1 January 2004 and 30 April 2008 yield a 90% confidence-level upper limit of $E_\nu^2 dN_{\nu_\tau}/dE_\nu < 9 \times 10^{-8}$ GeV cm^{-2} s^{-1} sr^{-1}.

DOI: 10.1103/PhysRevD.79.102001 PACS numbers: 95.55.Vj, 95.85.Ry, 98.70.Sa

I. INTRODUCTION

There are many efforts to search for high energy neutrinos with dedicated experiments [1–5]. Their observation should open a new window to the universe since they can give information on regions that are otherwise hidden from observation by large amounts of matter in the field of view. Moreover, neutrinos are not deviated by magnetic fields and, hence, they essentially maintain the direction of their production places. The existence of ultrahigh energy cosmic rays (UHECR) of energies exceeding 10^{19} eV makes it most reasonable to expect neutrino fluxes reaching similar energies. Although the origin of cosmic rays and their production mechanisms are still unknown [6], neutrinos are expected to be produced together with the cosmic rays and also in their interactions with the background radiation fields during propagation [7]. Unfortunately there are still many unknowns concerning cosmic ray origin and neutrino fluxes remain quite uncertain. Because of their relation to cosmic ray production and transport, the detection of UHE neutrinos should in addition give very valuable information about cosmic ray origin.

Models of the origin and propagation of UHECR consider the production of pions decaying into neutrinos. If protons or nuclei of extragalactic origin are accelerated in extreme astrophysical environments their interaction with the matter or radiation fields in the source region should yield pions which decay giving rise to neutrino fluxes. In addition cosmic rays interact with the background radiation when traveling over long distances resulting in a steepening of the spectrum around 5×10^{19} eV. This is the Greisen-Zatsepin-Kuz'min (GZK) effect [8,9], consistent with the recently reported suppression of the cosmic ray flux above $\sim 4 \times 10^{19}$ eV [10,11] as well as the observed anisotropy of the highest energy cosmic rays and a possible correlation with relatively nearby extragalactic objects [12,13]. The GZK mechanism is a source of UHE neutrinos, in the case of protons through interactions with the cosmic microwave background (CMB) what gives rise to the cosmological neutrinos [14] and in the case of iron nuclei through interactions with infrared light that dissociates the nuclei. Alternative models, often referred to as *top-down* scenarios, have been developed although the latest limits on photon fractions [15] appear to discard them as an adequate explanation of the UHE cosmic rays. They are based on the decay of supermassive particles into leptons and quarks. The latter subsequently fragment into cosmic ray protons but pions dominate the fragmentation mechanism, their decays giving rise to photon and neutrino fluxes. The produced neutrinos would exceed those that can be expected by the cosmic ray interactions with the background fields and are typically produced with harder spectra.

Both conventional acceleration and top-down scenarios generate pions which decay to produce an electron to muon neutrino flavor ratio of order 1:2 while neutrinos of τ flavor are heavily suppressed at production. With the discovery of neutrino flavor oscillations [16] and maximal Θ_{23} mixing, the flavor balance changes as neutrinos propagate to Earth. After traveling cosmological distances approximately equal fluxes for each flavor are expected [17,18]. The idea of detecting ν_τ induced events through the emerging τ produced by neutrinos that enter the Earth just below the horizon, was presented for the first time in [19,20]. These Earth-skimming neutrinos undergo charged-current interactions to produce a very penetrating τ lepton. When the interaction occurs sufficiently close to the Earth's surface the τ can escape to the atmosphere and decay in flight. This would in most cases give rise to an extensive air shower traveling nearly horizontal and in the upward direction for an ideal spherical Earth's surface.

The Pierre Auger Observatory [21] has been designed to explore ultrahigh energy cosmic rays with unprecedented precision exploiting the two available techniques to detect UHE air showers, arrays of particle detectors, and fluorescence telescopes. It can also detect neutrinos by searching for deep inclined showers both with the surface detector [22] and with fluorescence telescopes [23]. Showers resulting from τ decays induced by Earth-skimming neutrinos can also be detected with the Pierre Auger Observatory, both with the surface and the fluorescence detectors. This channel has been shown to increase the possibilities for detecting neutrinos and, in particular, using the surface detector of the Pierre Auger Observatory which becomes most sensitive to neutrinos in the EeV range [24].

An upper limit on the diffuse flux of τ neutrino of $E_\nu^2 dN_{\nu_\tau}/dE_\nu < 1.3 \times 10^{-7}$ GeV cm^{-2} s^{-1} sr^{-1} at 90% C.L. was reported in [25] using data collected between 1 January 2004 and 31 August 2007 with the surface detector of the Pierre Auger Observatory. The collected data were searched for τ neutrino candidates applying a ν_τ identification criterion that was obtained simulating Earth-skimming ν_τs, their interactions in the Earth, propagation of the subsequent τ leptons, and the associated showers they produce in the atmosphere. This article discusses in detail the search procedure to discriminate UHE Earth-skimming τ neutrinos used in [25] as well as the compute

of the exposure and the evaluation of the systematics. This article also uses an updated data sample. No candidates have been found in data from 1 January 2004 until 30 April 2008 and a new limit to the diffuse flux of UHE ν_τ is presented. The article is organized as follows. In Sec. II, the Pierre Auger Observatory is briefly described. In Sec. III, the needed Monte Carlo simulations are detailed. In Sec. IV, the method for discriminating neutrino-induced showers is explained and the selection procedure is presented. In Sec. V, the computation of the exposure is reported. In Sec. VI, the systematic uncertainties are discussed. In Sec. VII, the results from the Pierre Auger Observatory data for ν_τ Earth-skimming neutrinos are shown. Finally in Sec. VIII, this work is summarized.

II. THE PIERRE AUGER OBSERVATORY

The Pierre Auger Observatory will consist of two hybrid detectors in the northern and southern hemispheres, each one combining an array of particle detectors and fluorescence telescopes for redundancy and calibration [26]. The Southern Observatory is in Malargüe, Mendoza, Argentina and its construction phase is currently completed. It covers 3000 km^2 with regularly spaced particle detectors and with four fluorescence eyes at the perimeter that overlook the same area [21]. There are plans to construct the Northern Auger Observatory in Lamar, Colorado, USA [27]. Data have been taken with the Southern Pierre Auger Observatory since January 2004 while it was under construction. The amount of data that has been accumulated for the analysis described in this article corresponds to about 1.5 times the data that will be gathered in a whole year with the complete detector. This article will only address the search for Earth-skimming neutrinos with the array of particle detectors that constitutes the surface detector of the Southern Pierre Auger Observatory.

A. The surface array of the Pierre Auger Observatory

The Southern surface detector (SD) consists of 1600 Cherenkov water tanks (3.6 m diameter and 1.2 m high) arranged in a triangular grid with 1.5 km spacing between them, covering an almost flat surface, at an approximate altitude of 1400 m above sea level. Each tank is a polyethylene tank internally coated with a diffusive Tyvek^{TM} liner filled with 12 tons of purified water. The top surface has three photo multiplier tubes (PMTs) in optical contact with the water in the tank. The PMT signals are sampled by 40 MHz flash analog digital converters (FADC). Each tank is regularly monitored and calibrated in units of vertical equivalent muons (VEM) corresponding to the signal produced by a μ traversing the tank vertically [28]. The system transmits information by conventional radio links to the Central Data Acquisition System (CDAS) located in Malargüe. The PMTs, a local processor, a GPS receiver, and the radio system are powered by batteries with solar panels. Once installed, the local stations work continuously without external intervention.

The local trigger at the level of an individual Cherenkov tank (second order or T2 trigger) is the logical *OR* of two conditions: either a given threshold signal (1.75 VEM) is passed in at least one time bin of the FADC trace, or a somewhat lower threshold (0.2 VEM) is passed at least in 13 bins within a 3 μs time window (120 bins) [29]. The latter condition, the so-called *time over threshold* (ToT), is designed to select broad signals in time, characteristic of the early stages of the development of an extensive air shower (EAS). The data acquisition system receives the local triggers and builds a global trigger requesting a relatively compact configuration of three local stations compatible in time, each satisfying the ToT trigger, or 4 triggered stations with any T2 trigger (a third level or T3 trigger) [30]. With the complete array, the global T3 trigger rate will be about three events per minute, one third being actual shower events at energies above 3×10^{17} eV.

B. The data sample

The SD has been taking data in a stable manner since January 2004 [31]. Meanwhile the array has been growing and the number of deployed stations has increased from 120 to 1600 during the period analyzed in this article.

The analysis reported here is restricted to selected periods in order to eliminate inevitable problems associated to the construction phase, typically in the data acquisition, in the communication system and due to hardware instabilities. To ensure the quality of the data, we have analyzed the arrival time of the events under the reasonable hypothesis that the rate of physics events recorded by the detector (after proper size normalization) is independent of time. Given the large aperture of the SD and the level at which anisotropies could exist on the sky [32] this approximation is, from this point of view, well justified. Assuming a constant rate λ of physics events, the probability P of the time interval t between two consecutive events to be larger than T is given by

$$P(t > T) = e^{-\lambda T}, \tag{1}$$

where the value of λ is the mean rate of the recorded events normalized to the detector size.

Consecutive events for which P is below a certain threshold value $P_{\rm cut}$ are assumed to belong to periods with problems in the data acquisition and are used to define the bad periods to be rejected. The procedure will reject a good period with probability $P_{\rm cut}$ together with the eventual bad ones. So in principle one would like $P_{\rm cut}$ to be as small as possible. The choice of $P_{\rm cut}$ is made by finding where the distribution of probability of the time interval between two consecutive events differs from being flat. The numerical value of $P_{\rm cut}$ was found to be $\sim 10^{-5}$, which allows us to reject only a small fraction of good periods while removing the periods that lead to a nonflat probabil-

ity. When data taking began, the bad periods were of the order of 10% of the operating time but by the end of the time period considered in this work we were typically below 1% [33].

Once the bad periods have been removed, the events that have passed the third level trigger [30] from January 2004 until April 2008 constitute the data sample used in this paper.

III. END TO END SIMULATION CHAIN

In order to obtain a flux or a flux limit from the data, the detector neutrino showers have to be searched with a selection criterion and the exposure of the detector must be accordingly computed. Both the criteria to identify neutrino-induced showers and the computation of the exposure to ν_τ are based on Monte Carlo techniques. Three separate simulations can be identified. First a dedicated simulation that deals with the neutrinos entering the Earth and the τ leptons that exit. A second simulation involves the τ decay in flight and the development of an up-going atmospheric shower. Finally a simulation of the tank response to the through-going particles is performed to convert the particles at ground level obtained in the shower simulation to an actual detector signal.

A. Earth-skimming neutrinos

As Earth-skimming ν_τs penetrate the Earth they interact to produce τ leptons that suffer energy loss but can escape the Earth and decay in the atmosphere. As a result the incoming neutrinos give rise to an emerging τ flux which depends on the depth of matter traversed (for a spherical Earth as assumed here, it depends only on the nadir angle). The decay of the τ lepton in the atmosphere induces an EAS that can trigger the SD. The efficiency of this conversion plays a key role in the calculation of the detector exposure. The τ flux has been computed using simulation techniques that take into account the coupled interplay between the τ and the ν_τ fluxes as they traverse large matter depths through charged-current (CC) weak interactions and through τ decay. Energy losses induced by neutral current (NC) interactions for both particles are taken into account as a stochastic process. The energy losses through bremsstrahlung, pair production, and nuclear interactions for the τ lepton are applied continuously, which, at the level of accuracy we need for this work, is a reasonably good approximation [34].

Propagation of particles through matter is performed in small depth steps. At each step the particles are followed and the probability for interaction and decay (in the case of the τ) are evaluated taking into account the particle energy. The chain starts with an incident ν_τ which may interact by CC or NC. When the former occurs, a τ lepton is generated, and its energy is selected taking into account the y distribution of the interaction, where y is the fraction of the ν_τ energy transferred to the nucleon in the laboratory frame. If the ν_τ interacts through a NC its energy is computed taking the y distribution into account. Once a τ lepton is produced, it can undergo energy loss, weak interactions both neutral and charged, and decay. In the case of CC interaction or decay a new ν_τ is produced which regenerates the ν_τ flux that is propagated further. Finally, if a τ lepton emerges from Earth, its energy, direction, and decay position are stored and used as an input for the simulation of atmospheric showers induced by τ leptons.

For the relevant depths inside the Earth where τ leptons can be produced and reach the surface (few km) a homogeneous density of $2.65\ \mathrm{g\,cm^{-3}}$ can be assumed. Parametrizations of the cross section for weak interactions and for the y distributions at very high energy are used. The cross section for CC interactions is taken from [35] and the y distribution from [36]. For NC interactions, the cross section is assumed to be 0.4 that of the CC [37]. The energy losses for τ leptons are parametrized following case III in [38], which gives the best representation of Monte Carlo simulation.

B. Extensive air showers in the atmosphere

The τ decays in the atmosphere give rise to secondaries that may initiate an EAS that can trigger the SD. The decay mode has been simulated using the TAUOLA package version 2.4 [39] to obtain the type of the secondaries and their energies which are subsequently injected in AIRES (version 2.6.0) [40] with SIBYLL 2.1 [41] as a model for the hadronic interactions at high energy. Showers induced by up-going τs with energies from $\log(E\tau/\mathrm{eV}) = 17$ to 20.5 in steps of 0.5 have been simulated at zenith angles ranging between 90.1° and 95.9° in steps of 0.01 rad and at an altitude above the Pierre Auger Observatory that ranges from 0 m to 2500 m in 100 m steps. Ten showers have been generated for each combination of energy, zenith angle, and altitude, which leads to a total of 20 000 showers.

The extremely large amount of particles involved in an ~EeV shower makes it impractical to follow all the secondaries. The current simulation packages include a statistical sampling algorithm based on the thinning algorithm originally introduced in [42]. Only a small representative fraction of the total number of particles is propagated. Statistical weights are assigned to sampled particles in order to compensate for the rejected ones.

C. Detector response

The first step in the detector simulation is to obtain the particles reaching each tank from the sampled particles produced in the simulation of the EAS. A resampling algorithm is necessary to convert the output of the program to the expected number of particles that enter a SD station. This is done averaging over an area around the station that is large enough to avoid unphysical fluctuations from the thinning procedure, and at the same time small enough to avoid large differences in the density and average proper-

ties of particles in different places on the area [43]. Each particle reaching the station is injected inside the tank, and a detailed simulation is performed to obtain the light hitting the PMTs as a function of time. The simulated FADC traces are obtained as the superposition of the signal of all individual particles entering the tank accounting for their arrival time. Finally both the local and central trigger algorithms are applied and the event is stored in the same format as data [44].

At the highest simulated values of incident angles or altitudes where the τ decays, none of the simulated showers at any of the simulated energies fulfills the central trigger conditions. This is taken as a clear indication that a complete sample of showers has been produced without introducing any bias and that it therefore correctly represents the characteristic τ showers that could trigger the SD detector.

IV. DISCRIMINATION OF NEUTRINO-INDUCED SHOWERS

A. Neutrino signature: inclined showers in the early stages

UHE particles interacting in the atmosphere give rise to a shower with an electromagnetic component reaching its maximal development after a depth of the order of 800 g cm^{-2} and extinguishing gradually within the next 1000 g cm^{-2}. After roughly a couple of vertical atmospheric depths only high energy muons survive. In the first stages of development, while the electromagnetic component develops, the time spread of the particles in the shower front is large ($\sim \mu s$). When the shower becomes old, most of the particles in the shower front, the high energy muons, arrive in a short time window (~ 100 ns). As a consequence very inclined showers induced by protons or nuclei (or possibly photons) in the upper atmosphere reach the ground as a thin and flat front of muons accompanied by an electromagnetic halo, which is produced by bremsstrahlung, pair production, and muon decays, and has a time structure very similar to that of the muons. On the other hand, if a shower is induced by a particle that interacts deep in the atmosphere (a deep neutrino interaction in air, or a tau decay), its electromagnetic component could hit the ground and give a distinct broad signal in time. The signal in each station of the SD is digitized using FADCs, allowing us to unambiguously distinguish the narrow signals from the broad ones and thus to discriminate stations hit by an EAS in the early stages of development or by an old EAS. This is illustrated in Fig. 1 where we show FADC traces from two different real events. The FADC trace taken from the shower with a zenith angle of 22° is representative of an EAS in the early stages while the other is representative of an old EAS.

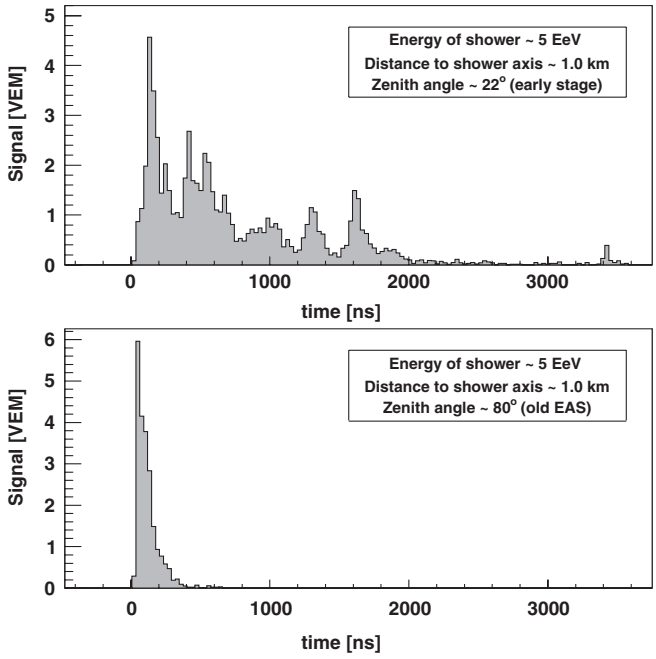

FIG. 1. FADC traces of stations at 1 km from the shower core for two real showers of 5 EeV. Top panel: early stages of development ($\theta \sim 22°$); bottom: old extensive air shower ($\theta \sim 80°$).

B. Identification of neutrino candidates

The identification of showers induced by Earth-skimming τ neutrinos implies searching for very inclined (quasihorizontal) showers in an early stage of development. Broad signals, which are characteristic as long as the electromagnetic component still develops, produce a ToT local trigger (see Sec. II A). A bunch of muons from cosmic ray showers can produce high amplitude signals extended in time or two independent muons can arrive inside the given time interval. Both would also produce a ToT local trigger which is not associated to the presence of electromagnetic component from a neutrino shower. To get rid of them, a further requirement is made to the signals in order to filter out these backgrounds. First a cleaning of the FADC trace is done to remove segments of the trace that could be generated by an accidental muon arriving closely before or after the shower front. Segments of the FADC trace are defined by neighbor bins above 0.2 VEM, allowing gaps of up to 20 bins and only the segment with the largest signal is kept. An *offline ToT* is defined by requiring that the signal after cleaning (the segment with largest signal) of the FADC trace has at least 13 bins above the low threshold (0.2 VEM) and the ratio of the integrated signal over the peak height exceeds by a factor 1.4 the average ratio observed in signals of isolated particles (as defined in the calibration procedure [28]). The central trigger conditions are applied only to stations that fulfill the offline ToT. Still a small number of nucleonic showers with a large number of triggered tanks may have a subsample of stations that satisfy this condition even if in all

the other stations the signal is not broad at all. In order to reject such events, at least 60% of the triggered stations are required to fulfill the offline ToT. After this selection procedure, an almost pure sample of showers reaching the ground at their early stages is selected.

Once the criterion for young showers is established a second criterion must be used to select very inclined showers as expected from Earth-skimming neutrino interactions. The devised method uses two variables associated to the *footprint* that the triggered tanks of the event leave on the ground and the apparent speed with which the signal *moves* across the array. First a symmetric tensor is built using the station signals included in the central trigger and their ground positions (analogous to the tensor of inertia of a mass distribution, see Eq. (2)),

$$\begin{aligned} S &= \Sigma_i s_i, \qquad \langle X\rangle = \Sigma_i s_i x_i/S, \qquad \langle Y\rangle = \Sigma_i s_i y_i/S, \\ I_{xx} &= \Sigma_i s_i (x_i - \langle X\rangle)^2/S, \qquad I_{yy} = \Sigma_i s_i (y_i - \langle Y\rangle)^2/S, \\ I_{xy} &= I_{yx} = \Sigma_i^n s_i (x_i - \langle X\rangle)(y_i - \langle Y\rangle), \end{aligned} \tag{2}$$

where s_i is the signal in VEM for each station; (x_i, y_i) are the coordinates of each station; and Σ_i is the sum over the stations.

The corresponding major and minor axes are used to define a characteristic *length* and a *width* of the pattern as the square root of the eigenvalues of the symmetric tensor (see Eq. (3)),

$$\begin{aligned} \text{length}^2 &= \frac{I_{xx} + I_{yy} + \sqrt{(I_{xx} - I_{yy})^2 + 4I_{xy}^2}}{2S}, \\ \text{width}^2 &= \frac{I_{xx} + I_{yy} - \sqrt{(I_{xx} - I_{yy})^2 + 4I_{xy}^2}}{2S}. \end{aligned} \tag{3}$$

Second for each pair of tanks (i, j), a *ground speed* is defined as $d_{i,j}/|\Delta t_{i,j}|$, where $d_{i,j}$ is the distance between the tanks (projected onto the major axis) and $|\Delta t_{i,j}|$ is the difference between the start times of their signals (Fig. 2). Quasihorizontal showers have an elongated shape (characterized by a large value of *length/width*) and they have ground speeds tightly concentrated around the speed of light c.

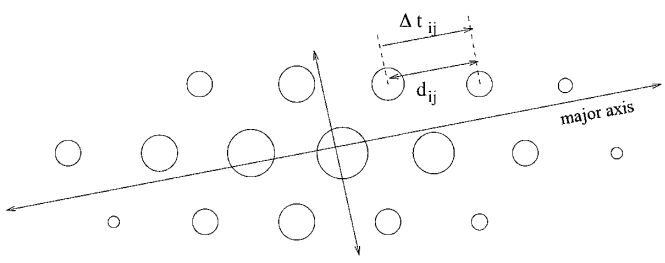

FIG. 2. Schematic view of the footprint of a shower on the SD array. Each circle represents the position of a station, and their sizes are proportional to the station signal.

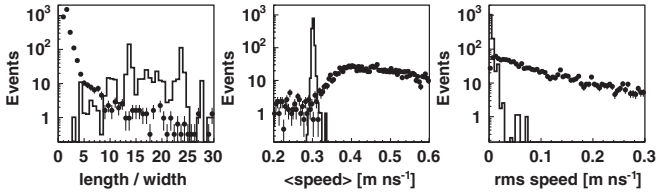

FIG. 3. Distribution of variables used to discriminate very inclined showers for an incident E^{-2} ν_τ flux (histogram), and for real events collected during November and December 2004 passing the *early stage* (see text) selection (points). Left panel: length/width; middle: average of the ground speed between pairs of stations; right: r.m.s. of the ground speeds.

In Fig. 3 the distributions of the two discriminating variables are shown for real events and simulated tau showers. Based on the comparison between MC simulations and data collected during November and December 2004, which is less than 1% of the used data sample, the following cuts were fixed to select Earth-skimming tau neutrino candidates:

(i) *length/width* >5
(ii) 0.29 m ns$^{-1}<$ average *ground speed* $<$0.31 m ns^{-1}
(iii) r.m.s. (*ground speed*) $<$0.08 m ns^{-1}

where the average *ground speed* and its dispersion are computed using only stations for which $|d_{i,j}|$ is larger than 1000 m.

Since the selection criteria relies on the shower footprint, we need to guarantee that a representative fraction of the event is detected with the SD. For this purpose the closest station to the center of the footprint (values $\langle X\rangle$ and $\langle Y\rangle$ defined in Eq. (2)) is required to be surrounded by at least five working stations at the time of occurrence of the event. Hence, events at the edges of the array with a small detected fraction of the footprint typically do not fulfill the selection criteria. This procedure is simple and robust. It can be applied to any footprint and does not require any global reconstruction.

V. NEUTRINO EXPOSURE OF THE SURFACE DETECTOR OF THE PIERRE AUGER OBSERVATORY

The next step in the calculation is to compute the exposure of the SD of the Pierre Auger Observatory to showers induced by UHE ν_τ. Each simulated Earth-skimming ν_τ event has to be tracked from the injection up to its identification through the defined selection cuts. The number of identified events is computed from the simulations of the EAS initiated by the secondaries in the tau decay and from the detector response to them. For a fixed energy of the τ (E_τ) and an infinite SD with all stations working, there is effectively only one relevant parameter determining the efficiency of trigger and identification: the altitude of the shower center (h_c). This is conveniently defined as the altitude of the shower axis at a distance of 10 km away

from the τ decay point along the shower axis (see Fig. 4). For the shower energies relevant in this analysis, h_c is very close to the altitude at which a horizontal shower has the largest lateral extension and is thus capable of producing the largest footprint at ground [24].

For a SD that covers a surface A, the aperture for a given neutrino energy (E_ν) can be expressed as follows:

$$\begin{aligned} Ap(E_\nu) &= \int A\cos\Theta d\Omega \int_0^{E_\nu} dE_\tau \int_0^\infty dh_c \left(\frac{d^2p_\tau(E_\nu)}{dE_\tau dh_c}\right)\epsilon_{ff} \\ &= 2\pi \int_{\pi/2+\alpha_m}^{\pi/2} A\cos\Theta\sin\Theta d\Theta \int_0^{E_\nu} dE_\tau \\ &\quad \times \int_0^\infty dh_c \left(\frac{d^2p_\tau(E_\nu)}{dE_\tau dh_c}\right)\epsilon_{ff} \\ &= \pi A \sin^2\alpha_m \int_0^{E_\nu} dE_\tau \int_0^\infty dh_c \left(\frac{d^2p_\tau(E_\nu)}{dE_\tau dh_c}\right)\epsilon_{ff}, \quad (4) \end{aligned}$$

where $d^2p_\tau/(dE_\tau dh_c)$ is the differential probability of an emerging τ as a function of energy and altitude for a fixed incident ν_τ energy, that can be easily obtained folding the simulations described in Sec. III A for the emerging τs with the tau decay probability as a function of flight distance. ϵ_{ff} is the probability to identify a τ (including the trigger efficiency), that is assumed to depend only on E_τ and h_c. The integral in Θ is done from $\pi/2 + \alpha_m$ rad ($\alpha_m = 0.1$ rad) to $\pi/2$ rad since an incident ν_τ with a greater angle has no chance to produce an emerging τ that produces an observable shower at ground level. The latter integration can be performed by the Monte Carlo technique as described in Sec. III, leading to

$$Ap(E_\nu) = \pi A \sin^2\alpha_m \frac{\sum_i \epsilon_{ff}(E_\tau^{(i)}, h_c^{(i)})}{N_{\rm sim}}, \quad (5)$$

where $N_{\rm sim}$ is the number of simulated events. In Fig. 5, the trigger and identification efficiencies for an ideal (no holes and no malfunctioning stations) and infinite array are shown as given by the simulated EAS described in Sec. III B. They have been calculated by throwing once each simulated EAS on the detector array with a random core position. The maximum efficiency that can be reached

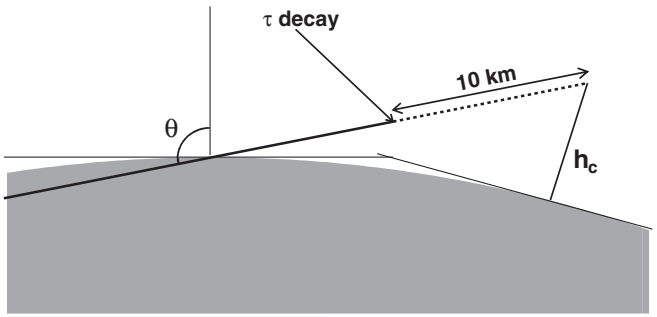

FIG. 4. Geometry of the induced τ shower with the definition of the parameters, h_c and Θ, involved on the exposure computation (see text). Angles and distances are not proportional. They have been exaggerated to help the readability of the figure.

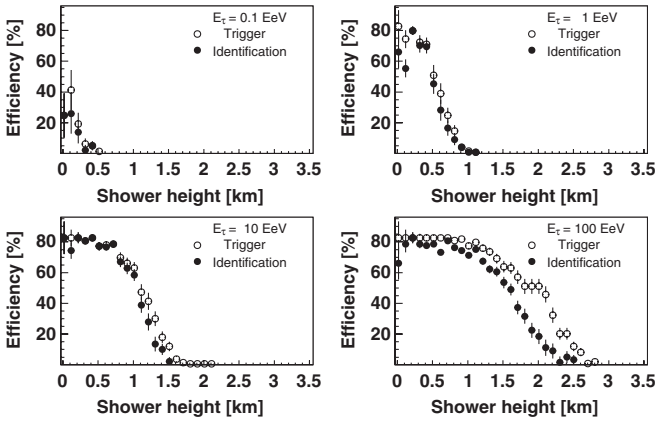

FIG. 5. Trigger (open dots) and identification (closed dots) efficiency as a function of the height above ground of the shower at 10 km from the decay point. The efficiency is shown for MC showers induced by τs with energy of 0.1 (top-left), 1 (top-right), 10 (bottom-left), and 100 (bottom-right) EeV merging all zenith angles.

is 82.6% due to the μ channel decay [45]. This decay mode does not produce a detectable shower neglecting the possibility of hard muon bremsstrahlung or pair production near the detector which should have a negligible effect on the final limit. The identification efficiency depends smoothly on E_τ and h_c, and hence it can be safely interpolated.

During the period of data taking considered in this work, the SD of the Pierre Auger Observatory has been growing continuously. It is of course mandatory to take into account this evolution, as well as the instabilities of each station. Therefore Eq. (5) is not valid to compute the actual SD array. Instead the following expression can be used:

$$\begin{aligned} Ap(E_\nu, t) = \pi \sin^2\alpha_m \int_0^{E_\nu} dE_\tau \int_0^\infty dh_c \Bigg(\frac{d^2p_\tau}{dE_\tau dh_c} \\ \times \int_S dxdy \epsilon_{ff}(E_\tau, h_c, x, y, A_{\rm Conf}(t))\Bigg), \quad (6) \end{aligned}$$

where ϵ_{ff} now also depends on the position of the shower in the array (x, y), and on the instantaneous configuration of the array at time t denoted here as $A_{\rm Conf}(t)$. The integral over the area S includes the whole SD array.

Hence, the total exposure during the considered period of data taking is the time integration of the instantaneous aperture given by

$$\begin{aligned} Exp &= \int dt Ap(E_\nu, t) \\ &= \pi \sin^2\alpha_m \int_0^{E_\nu} dE_\tau \int_0^\infty dh_c \left(\frac{d^2p_\tau}{dE_\tau dh_c}\bar{B}_\tau\right) \\ &\quad \times \bar{B}_\tau\Big(E_\tau, h_c\Big) = \int_T dt \int_S dxdy \epsilon_{ff}(E_\tau, h_c, x, y, A_{\rm Conf}(t))\Big). \end{aligned} \quad (7)$$

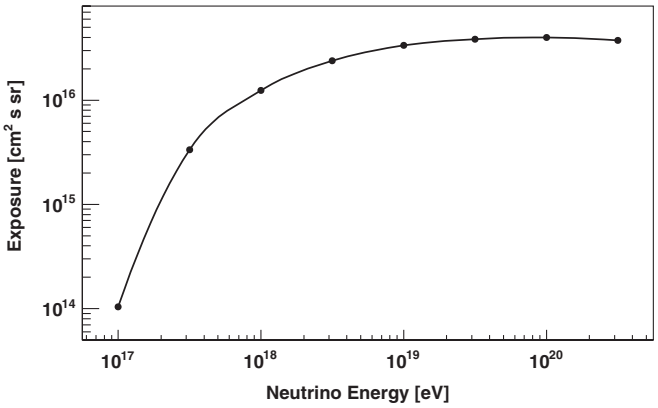

FIG. 6. Earth-skimming neutrino exposure of the Pierre Auger Observatory accumulated from January 2004 until April 2008. All the identification cuts described in Sec. IV B are taken into account.

The exposure is computed by Monte Carlo in two independent steps. First, the integrals in t and (x, y) are computed using the simulations of the EAS and the detector. The number of working stations and their status are monitored every second allowing us to know with very good accuracy the instantaneous SD configuration [46]. For each simulated EAS, several random times from January 2004 until April 2008 excluding the rejected periods are selected. The number of random times is selected in a monthly base to ensure a statistical precision on the exposure at 1% level. For each time, the evaluation of the identification efficiency is done for any position of the shower in the SD array. The average over all showers with the same E_τ and h_c gives the integral in time and area of ϵ_{ff}, allowing one to compute $\bar{B}_\tau(E_\tau, h_c)$. The second step computes the integral in h_c and E_τ as in the case of a perfect array. The estimated uncertainty of this method given the Monte Carlo simulations is below 3%. The accumulated exposure is shown in Fig. 6. It corresponds to an equivalent time of about 1.5 years of the complete SD array (1600 water tanks).

VI. SYSTEMATIC UNCERTAINTIES

Several sources of systematic uncertainty have been carefully considered. They are addressed below. We have chosen as a reference the aperture calculated with ν cross section from Ref. [35], the parametrization of the energy losses from Ref. [38], a uniform random distribution for the τ polarization, a spherical model of the Earth, and the SIBYLL [41] hadronic model in combination with AIRES shower simulator [40]. The systematic uncertainties in this section are all quoted with respect to this aperture and therefore in general asymmetric. Moreover, to be able to quote a range for the systematic uncertainties independently of the energy, an E^{-2} incident flux of neutrinos has been assumed.

First, the location of the Pierre Auger Observatory is close to the Andes and not very far away from the Pacific. The actual topography of the Pierre Auger Observatory can be taken into account by a detailed Monte Carlo simulation [47]. The effect of the Andes on the expected event rate has been studied with the aid of a digital elevation map available from the Consortium for Spatial Information [48]. The number of detected events decreases by 18% if Andes are neglected. Conservatively and for consistency with [25], this effect is included on the systematic uncertainties instead of using the elevation map to compute the reference aperture.

There is quite some level of uncertainty in EAS simulation because accelerator data have to be extrapolated to the shower energies under discussion. However these uncertainties are not expected to have a large effect on the final result since the electromagnetic component of the shower, which is the most relevant part for neutrino identification, is believed to be better reproduced by simulations. Shower simulations have been done with two hadronic models (QGSJET [49] and SIBYLL [41]) and passed through two different detector simulations. Potential biases due to the limited statistic of simulated showers and the used thinning level [42] have also been checked. Based on all that, systematic uncertainties of $^{+20\%}_{-5\%}$ are quoted as due to the Monte Carlo simulation of both the EAS[1] and the detector [44], the former being the main contribution. The simulations of the interactions inside the Earth have been extensively checked by comparison with an analytical calculation [51], an iterative solution of the transport equations [52], and several independent simulations. The uncertainty associated to this simulation process itself is expected to be below the 5% level.

Monte Carlo simulations also make use of several physical magnitudes that have not been experimentally measured at the relevant energy range, namely: the ν cross section, the τ energy losses, and the polarization of the τ. All of them can be computed in the framework of the standard model of particle physics using the parton distribution functions (PDFs).

The allowed range for the ν cross section due to uncertainties in the PDFs has been studied in [35] and includes both the effects of the experimental uncertainties on the PDFs fitted to ZEUS and fixed target data evolved at next-to-leading order [53], as well as theoretical uncertainties in the implementation of heavy quark masses on the PDF evolution. For the purpose of this study, the ZEUS PDFs and their uncertainties were recalculated [35] using

[1]Currently, QGSJET and SIBYLL are the only hadronic models available to be used with the used EAS simulation package. Other recently introduced models like EPOS [50] are not yet available to test their effect. Although, in the case of EPOS, due to the large number of muons, and the flatter lateral distribution the trigger efficiency should be larger and in this respect our limit should be conservative.

the DGLAP equations throughout the relevant kinematic range (down to $x \sim 10^{-12}$). This leads to a $^{+5\%}_{-9\%}$ systematic uncertainty for the number of ν expected to be detected by the SD of the Pierre Auger Observatory.

The decay of the τ lepton plays a key role on the whole Monte Carlo simulation. Both the branching ratios of the different decay modes and the energy distribution among the products are important. The latter depends on the τ polarization, which in turn depends on the PDFs. The most and least favorable cases in the range of possible polarizations (helicity ± 1) have been used to estimate the uncertainty associated to it. The use of the extreme cases of polarization of the τ will not produce more than $^{+17\%}_{-10\%}$ differences on the exposure.

Finally, energy losses include τ bremsstrahlung (BS) and pair production (PP) as well as nuclear interactions. The contributions from BS and PP can be accurately rescaled from the values for muons [45,54]. The nuclear contribution comes from the photonuclear cross section and it is much more uncertain. The differential photonuclear cross section as a function of the PDFs has been given in [55,56]. There exist estimates of the tau energy losses for the relevant energy range based on them [23,38,55–57]. Different calculations of the energy losses may lead up to $^{+25\%}_{-10\%}$ systematic uncertainties in the exposure.

In Fig. 7 the exposure for one year of the SD array with 1600 water tanks is shown in the most and least favorable cases of the systematic uncertainties previously discussed. The systematic uncertainties do not have the same effect for all ν_τ energies. The importance of each different contribution to the global systematic uncertainty in the exposure is neither the same at all ν_τ energies. At low energies (~ 1 EeV) the τ polarization, the ν cross section, and the τ energy losses dominate. At higher energies those contributions become smaller and others increase. The latter comes from neglecting the mountains, the effect of which increases with the ν_τ energy. The small depth traversed

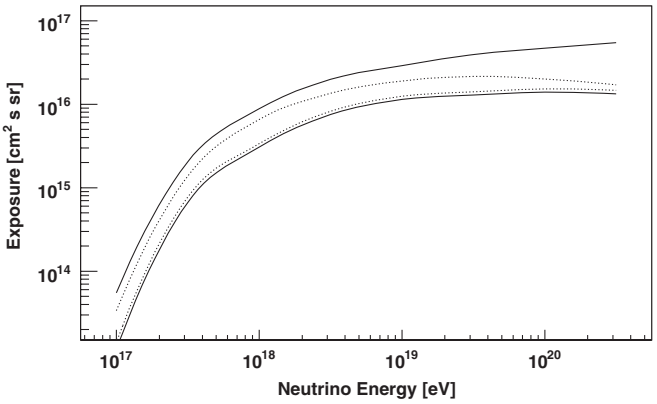

FIG. 7. The Pierre Auger Observatory exposure for one year of a full SD array data. Solid lines bracket the total systematic uncertainty, while the dotted ones only bracket the allowed range of polarizations, ν cross sections, and energy loss uncertainties.

TABLE I. Ratio of expected number of ν_τ for either GZK-like or for E^{-2} incident spectra in the most and least favorable scenarios for each source of systematic uncertainties.

Source	Factor
EAS Simulations	1.30
Topography	1.18
Tau polarization	1.30
Cross section	1.15
Energy losses	1.40
Total	2.9

becomes more relevant due to the larger cross section. The former is due to the contribution from the ν cross section uncertainties. A larger cross section increases the interaction probability for the neutrinos but reduces the solid angle due to the flux absorption in the Earth. This makes the uncertainty in the cross section to contribute mainly around 1 EeV.

The effect of the systematic uncertainties on the expected rate of identified ν_τ will depend on the shape of the actual incident ν_τ flux. The effect is almost the same either for GZK-like fluxes or for E^{-2} fluxes, giving a factor ~ 3 for the systematic uncertainty in either case (see Table I). Moreover, the energy dependent effect also produces differences on the energy range where most of the identified ν_τ are expected. For instance, if an E^{-2} flux is assumed the energy range where 90% of the events are expected changes from 0.22–23 EeV in the least favorable scenario to 0.20–26 EeV in the most favorable one.

The relevant range of PDFs involved in both the ν_τ and the τ photonuclear cross sections includes combinations of Bjorken-x and Q^2 where no experimental data is available. Only extrapolations that follow the behavior observed in the regions with experimental data have been considered. Different extrapolations to low x and high Q^2 would lead to a wide range of values for the ν cross section as well as for the τ energy losses. The systematic uncertainties due to this have not been included in the quoted systematics. Possible large ν cross sections have not been taken into account either.

VII. SEARCH RESULTS AND NEUTRINO LIMIT

The measurement of the spectral shape or energy dependent upper limits on ν_τ are out of the reach of the Pierre Auger Observatory scope for mainly three reasons. First, the generic energy reconstruction algorithms developed for conventional nucleonic showers do not work if the position of the shower axis is not determined (here, a knowledge of the altitude at which the shower is produced would be needed); second, the fraction of τ energy contributing to the EAS depends on the decay mode; and finally, the energy transferred from the incident ν_τ to the emerging τ is not known. At best an approximate lower bound of the initial ν_τ energy could be obtained.

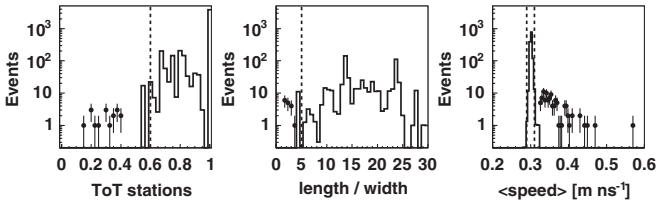

FIG. 8. Distribution of discriminating variables for an incident E^{-2} ν_τ flux (histogram) and for the real events (points). Events that survive all the selection cuts except the one for the shown variable are used. The vertical lines indicate the values to discriminate. Left panel: fraction of stations with a ToT signal; middle: length/width; right: average of the ground speed between pairs of stations.

The data have been searched for neutrino candidates over the analyzed data period and there are no events fulfilling the selection cuts. The events failing to pass only one of them have a quite different distribution for the discriminant parameter than the one of the simulated τ showers (see Fig. 8). In Table II, the number of events surviving after successive cuts for real data as well as the efficiencies for simulated ν_τs are shown. The huge reduction of events after selecting very inclined showers (elongated footprint and *ground speed*) reaching the ground in early stages (Young showers) is expected for showers induced by protons or nuclei (see Sec. IV A). The expected number of events surviving the combination of those cuts due to detector effects is also compatible with the observed discriminating power. Based on that, a limit for an injected spectrum $K \cdot \Phi(E)$ with a known shape $\Phi(E)$ can be derived. The 90% confidence level (CL), for 0 candidates and no background expected [58], on the value of K is

$$K_{90} = \frac{2.44}{\int \Phi(E) \cdot Exp(E) dE}, \tag{8}$$

where Exp is interpolated from Table III.

For an injected diffuse flux of ν_τ $dN/dE = K \cdot E^{-2}$, the 90% CL limit is $K_{90} = 6^{+3}_{-3} \times 10^{-8}$ GeV cm^{-2} s^{-1} sr^{-1}, where the uncertainties come from the systematics discussed in Sec. VI. The bound is obtained for the energy range $2 \times 10^{17} - 2 \times 10^{19}$ eV, with a systematic uncertainty of about 15%, over which 90% of the events can be expected for an E^{-2} flux.

TABLE II. Number of events passing the successive selection cuts. The Monte Carlo efficiency corresponds to identification efficiencies for νs of energy 1 EeV that trigger the SD detector. Data have been collected from January 2004 until April 2008.

Selection requirement	MC efficiency	Number of real events
Initial sample	1.00	3.97×10^6
Young showers	0.88	6.68×10^5
Elongated footprint	0.87	8.37×10^3
Ground speed $\sim c$	0.84	0
Contained footprint	0.76	0

TABLE III. Exposure of the SD of the Pierre Auger Observatory from January 2004 until April 2008. In the columns labeled highest and lowest we give the values of the exposure for the most optimistic and most pessimistic cases of the systematic uncertainties.

	Exposure [cm^2 s sr]	
$\log(E_\nu/\text{eV})$	Highest	Lowest
17.0	1.81×10^{14}	5.72×10^{12}
17.5	7.29×10^{15}	1.93×10^{15}
18.0	2.44×10^{16}	8.75×10^{15}
18.5	5.30×10^{16}	1.98×10^{16}
19.0	7.17×10^{16}	2.81×10^{16}
19.5	1.11×10^{17}	3.41×10^{16}
20.0	1.18×10^{17}	3.50×10^{16}
20.5	1.39×10^{17}	3.41×10^{16}

In Fig. 9, the limit for the *most pessimistic* scenario of systematic uncertainties is shown. It improves by a factor $\sim$3 in the most optimistic scenario (dotted line). Flux limits given by other experiments are also shown (divided by 3 if they are limits to all flavors to be able to compare): AMANDA [59,60], Baikal [61], RICE [62] (rescaled at 90% CL), HiRes [63,64], ANITA-lite [65], ANITA [66], GLUE [67], and FORTE [68]. For some of them the limits are given for an E^{-2} flux (integrated format), while for others the flux limit is given as $2.3/\text{Exposure} \cdot E_\nu$ (differential format). The limit from the ANITA-lite experiment

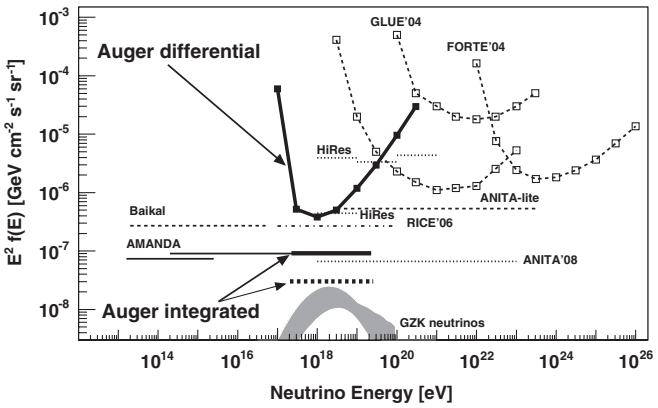

FIG. 9. Limits at 90% CL for *each flavor* of diffuse UHE neutrino fluxes assuming a proportion of flavors of 1:1 : 1 due to neutrino oscillations. The Auger limits are given using the most pessimistic case of the systematics (solid lines). For the integrated format, the limit that would be obtained in the most optimistic scenario of systematics is also shown (dashed line). See the text for the references to the other experimental limits. The shaded area corresponds to the allowed region of expected GZK neutrino fluxes computed under different assumptions [69–72], although predictions almost one order of magnitude lower and higher exist.

and the Pierre Auger Observatory are given in both formats for comparison. The differential format demonstrates explicitly that the sensitivity of the Pierre Auger Observatory to Earth-skimming neutrinos peaks in a narrow energy range close to where the GZK neutrinos are expected.

The energy range of the ν_τs explored with the Auger Observatory with this channel is very well suited to search for the diffuse flux of νs that are produced by the GZK effect.

VIII. SUMMARY AND PROSPECTS

The data set collected during the construction phase of the surface detector of the Pierre Auger Observatory from January 2004 until April 2008, is used to present an upper limit to the diffuse flux of ν_τ. The Earth-skimming technique together with the configuration of the surface detector gives the best sensitivity currently available around a few EeV, which is the most relevant energy to explore the predicted fluxes of GZK neutrinos. However in the worst case of systematic uncertainties, the limit presented here is still higher by about one order of magnitude than GZK neutrino predictions. The Pierre Auger Observatory will keep taking data for about 20 years over which the bound will improve by more than an order of magnitude if no neutrino candidate is found.

ACKNOWLEDGMENTS

The successful installation and commissioning of the Pierre Auger Observatory would not have been possible without the strong commitment and effort from the technical and administrative staff in Malargüe. We are very grateful to the following agencies and organizations for financial support: Comisión Nacional de Energía Atómica, Fundación Antorchas, Gobierno De La Provincia de Mendoza, Municipalidad de Malargüe, NDM Holdings and Valle Las Leñas, in gratitude for their continuing cooperation over land access, Argentina; the Australian Research Council; Conselho Nacional de Desenvolvimento Científico e Tecnológico (CNPq), Financiadora de Estudos e Projetos (FINEP), Fundação de Amparo à Pesquisa do Estado de Rio de Janeiro (FAPERJ), Fundação de Amparo à Pesquisa do Estado de São Paulo (FAPESP), Ministério de Ciência e Tecnologia (MCT), Brazil; AVCR AV0Z10100502 and AV0Z10100522, GAAV KJB300100801 and KJB100100904, MSMT-CR LA08016, LC527, 1M06002, and MSM0021620859, Czech Republic; Centre de Calcul IN2P3/CNRS, Centre National de la Recherche Scientifique (CNRS), Conseil Régional Ile-de-France, Département Physique Nucléaire et Corpusculaire (PNC-IN2P3/CNRS), Département Sciences de l'Univers (SDU-INSU/CNRS), France; Bundesministerium für Bildung und Forschung (BMBF), Deutsche Forschungsgemeinschaft (DFG), Finanzministerium Baden-Württemberg, Helmholtz-Gemeinschaft Deutscher Forschungszentren (HGF), Ministerium für Wissenschaft und Forschung, Nordrhein-Westfalen, Ministerium für Wissenschaft, Forschung und Kunst, Baden-Württemberg, Germany; Istituto Nazionale di Fisica Nucleare (INFN), Ministero dell'Istruzione, dell'Università e della Ricerca (MIUR), Italy; Consejo Nacional de Ciencia y Tecnología (CONACYT), Mexico; Ministerie van Onderwijs, Cultuur en Wetenschap, Nederlandse Organisatie voor Wetenschappelijk Onderzoek (NWO), Stichting voor Fundamenteel Onderzoek der Materie (FOM), Netherlands; Ministry of Science and Higher Education, Grant No. 1 P03 D 014 30, No. N202 090 31/0623, and No. PAP/218/2006, Poland; Fundação para a Ciência e a Tecnologia, Portugal; Ministry for Higher Education, Science, and Technology, Slovenian Research Agency, Slovenia; Comunidad de Madrid, Consejería de Educación de la Comunidad de Castilla La Mancha, FEDER funds, Ministerio de Ciencia e Innovación, Xunta de Galicia, Spain; Science and Technology Facilities Council, United Kingdom; Department of Energy, Contract No. DE-AC02-07CH11359, National Science Foundation, Grant No. 0450696, The Grainger Foundation USA; ALFA-EC/HELEN, European Union 6th Framework Program, Grant No. MEIF-CT-2005-025057, and UNESCO.

[1] M. Kestel (IceCube Collaboration), Nucl. Instrum. Methods Phys. Res., Sect. A **535**, 139 (2004).
[2] G. Aggouras *et al.*, Nucl. Instrum. Methods Phys. Res., Sect. A **552**, 420 (2005).
[3] R. Arnold *et al.*, Nucl. Instrum. Methods Phys. Res., Sect. A **536**, 79 (2005).
[4] J. Carr (ANTARES Collaboration), Nucl. Instrum. Methods Phys. Res., Sect. A **567**, 428 (2006).
[5] P. Miocinovic *et al.* (ANITA Collaboration), in *Proceedings of the 22nd Texas Symposium on Relativistic Astrophysics, Stanford*, econf C041213 (2004), p. 2516.
[6] For a review see for instance, A. V. Olinto, Phys. Rep. **333**, 329 (2000); P. Bhattacharjee and G. Sigl, Phys. Rep. **327**, 109 (2000); M. Nagano and A. A. Watson, Rev. Mod. Phys. **72**, 689 (2000); D. F. Torres and L. A. Anchordoqui, Rep. Prog. Phys. **67**, 1663 (2004); D. R. Bergman and J. W. Belz, J. Phys. G **34**, R359 (2007).
[7] For a review see for instance, T. K. Gaisser, F. Halzen, and T. Stanev, Phys. Rep. **258**, 173 (1995); **271**, 355(E) (1996);

J. G. Learned and K. Mannheim, Annu. Rev. Nucl. Part. Sci. **50**, 679 (2000); F. Halzen and D. Hooper, Rep. Prog. Phys. **65**, 1025 (2002); E. Waxman, New J. Phys. **6**, 140 (2004).
[8] K. Greisen, Phys. Rev. Lett. **16**, 748 (1966).
[9] G. T. Zatsepin and V. A. Kuzmin, JETP Lett. **4**, 78 (1966).
[10] R. Abbasi *et al.* (HiRes Collaboration), Phys. Rev. Lett. **100**, 101101 (2008)
[11] Pierre Auger Collaboration, Phys. Rev. Lett. **101**, 061101 (2008).
[12] Pierre Auger Collaboration, Science **318**, 938 (2007).
[13] Pierre Auger Collaboration, Astropart. Phys. **29**, 188 (2008).
[14] F. W. Stecker, C. Done, M. H. Salamon, and P. Sommers, Phys. Rev. Lett. **66**, 2697 (1991); **69**, 2738(E) (1992).
[15] Pierre Auger Collaboration, Astropart. Phys. **29**, 243 (2008).
[16] S. Fukuda *et al.*, Phys. Rev. Lett. **86**, 5656 (2001).
[17] J. G. Learned and S. Pakvasa, Astropart. Phys. **3**, 267 (1995).
[18] H. Athar *et al.*, Phys. Rev. D **62**, 103007 (2000).
[19] A. Letessier-Selvon, AIP Conf. Proc. **566**, 157 (2001).
[20] D. Fargion, Astrophys. J. **570**, 909 (2002).
[21] J. Abraham *et al.* (Pierre Auger Collaboration), Nucl. Instrum. Methods Phys. Res., Sect. A **523**, 50 (2004).
[22] K. S. Capelle *et al.*, Astropart. Phys. **8**, 321 (1998).
[23] C. Aramo *et al.*, Astropart. Phys. **23**, 65 (2005).
[24] X. Bertou *et al.*, Astropart. Phys. **17**, 183 (2002).
[25] Pierre Auger Collaboration, Phys. Rev. Lett. **100**, 211101 (2008).
[26] B. Dawson (Pierre Auger Collaboration), in *Proceedings of the 30th International Cosmic Ray Conference, Merida, 2007*, edited by R. Caballero, J. C. D'Olivo, G. Medina-Tanco, L. Nellen, F. A. Sánchez, and J. F. Valdés-Galicia (Universidad Nacional Autónoma de México, Mexico City, Mexico, 2008), p. 425.
[27] D. F. Nitz (Pierre Auger Collaboration), in *Proceedings of the 30th International Cosmic Ray Conference, Merida, 2007*, edited by R. Caballero, J. C. D'Olivo, G. Medina-Tanco, L. Nellen, F. A. Sánchez, and J. F. Valdés-Galicia (Universidad Nacional Autónoma de México, Mexico City, Mexico, 2008), p. 889.
[28] X. Bertou *et al.* (Pierre Auger Collaboration), Nucl. Instrum. Methods Phys. Res., Sect. A **568**, 839 (2006).
[29] D. Nitz (Pierre Auger Collaboration), IEEE Trans. Nucl. Sci. **51**, 413 (2004).
[30] D. Allard *et al.* (Pierre Auger Collaboration), in *Proceedings of the 29th International Cosmic Ray Conference, Pune* Vol. 7 (2005), p. 387.
[31] T. Suomijarvi (Pierre Auger Collaboration), in *Proceedings of the 30th International Cosmic Ray Conference, Merida, 2007*, edited by R. Caballero, J. C. D'Olivo, G. Medina-Tanco, L. Nellen, F. A. Sánchez, and J. F. Valdés-Galicia (Universidad Nacional Autónoma de México, Mexico City, Mexico, 2008), p. 311.
[32] E. Armengaud (Pierre Auger Collaboration), arXiv:0706.2640.
[33] Pierre Auger Collaboration (unpublished).
[34] O. Blanch Bigas *et al.*, Phys. Rev. D **77**, 103004 (2008).
[35] A. Cooper-Sarkar and S. Sarkar, J. High Energy Phys. 01 (2008) 075.
[36] A. Gazizov and M. P. Kowalski, Comput. Phys. Commun. **172**, 203 (2005).
[37] R. Gandhi *et al.*, Phys. Rev. D **58**, 093009 (1998).
[38] S. I. Dutta, Y. Huang, and M. H. Reno, Phys. Rev. D **72**, 013005 (2005).
[39] S. Jadach *et al.*, Comput. Phys. Commun. **76**, 361 (1993).
[40] S. J. Sciutto, Departamento de Fisica, Universidad Nacional de la Plata, available from http://www.fisica.unlp.edu.ar/auger/aires/, version 2.6.0 (2002).
[41] R. Engel *et al.*, in *Proceedings of the 26th International Cosmic Ray Conference, Utah* Vol. 1 (1999), p. 415.
[42] A. M. Hillas, in *Proceedings of the 17th International Cosmic Ray Conference, Paris* Vol. 8 (1981), p. 193.
[43] P. Billoir, Astropart. Phys. **30**, 270 (2008).
[44] P. Ghia (Pierre Auger Collaboration), in *Proceedings of the 30th International Cosmic Ray Conference, Merida, 2007*, edited by R. Caballero, J. C. D'Olivo, G. Medina-Tanco, L. Nellen, F. A. Sánchez, and J. F. Valdés-Galicia (Universidad Nacional Autónoma de México, Mexico City, Mexico, 2008), p. 315.
[45] W. M. Yao *et al.* (Particle Data Group), J. Phys. G **33**, 1 (2006).
[46] D. Allard *et al.* (Pierre Auger Collaboration), in *Proceedings of the 29th International Cosmic Ray Conference, Pune* Vol. 7 (2005), p. 71.
[47] D. Gora, M. Roth, and A. Tamburro, Astropart. Phys. **26**, 402 (2007).
[48] Consortium for Spatial Information (CGIAR-CSI), http://srtm.csi.cgiar.org/.
[49] N. N. Kalmykov *et al.*, Nucl. Phys. B, Proc. Suppl. **52**, 17 (1997).
[50] K. Werner and T. Pierog, AIP Conf. Proc. **928**, 111 (2007).
[51] E. Zas, New J. Phys. **7**, 130 (2005).
[52] O. Blanch-Bigas *et al.*, Phys. Rev. D **78**, 063002 (2008).
[53] S. Chenakov *et al.* (ZEUS Collaboration), Phys. Rev. D **67**, 012007 (2003).
[54] A. Van Ginneken, Nucl. Instrum. Methods Phys. Res., Sect. A **251**, 21 (1986).
[55] S. I. Dutta, M. H. Reno, I. Sarcevic, and D. Seckel, Phys. Rev. D **63**, 094020 (2001).
[56] E. V. Bugaev and Yu. V. Shlepin, Phys. Rev. D **67**, 034027 (2003).
[57] E. Bugaev, T. Montaruli, Y. Shlepin, and I. Sokalski, Astropart. Phys. **21**, 491 (2004).
[58] G. J. Feldman and R. D. Cousins, Phys. Rev. D **57**, 3873 (1998).
[59] A. Achterberg (IceCube Collaboration), Phys. Rev. D **76**, 042008 (2007).
[60] M. Ackermann *et al.* (IceCube Collaboration), Astrophys. J. **675**, 1014 (2008).
[61] V. Aynutdinov *et al.* (BAIKAL Collaboration), Astropart. Phys. **25**, 140 (2006).
[62] I. Kravchenko *et al.*, Phys. Rev. D **73**, 082002 (2006).
[63] K. Martens (HiRes Collaboration), arXiv:0707.4417.
[64] R. U. Abbasi *et al.*, arXiv:0803.0554.
[65] S. W. Barwick *et al.* (ANITA Collaboration), Phys. Rev. Lett. **96**, 171101 (2006).
[66] P. W. Gorham *et al.* (ANITA collaboration), arXiv:0812.2715.
[67] P. W. Gorham *et al.*, Phys. Rev. Lett. **93**, 041101 (2004).
[68] N. G. Lehtinen, P. W. Gorham, A. R.Jacobson, and R. A.

Roussel-Dupre, Phys. Rev. D **69**, 013008 (2004).
[69] D. Allard *et al.*, J. Cosmol. Astropart. Phys. 09 (2006) 005.
[70] R. J. Protheroe, Nucl. Phys. B, Proc. Suppl. **77**, 465 (1999).
[71] R. Engel, D. Seckel, and T. Stanev, Phys. Rev. D **64**, 093010 (2001).
[72] L. A. Anchordoqui *et al.*, Phys. Rev. D **76**, 123008 (2007).